Published in final edited form as:
Eur J Immunol. 2013 July ; 43(7): 1873–1882. doi:10.1002/eji.201243214.

Prevention of F-actin assembly switches the response to SCF from chemotaxis to degranulation in human mast cells

Daniel Smrž[1,**], **Geethani Bandara**[1], **Michael A. Beaven**[2], **Dean D. Metcalfe**[1], and **Alasdair M. Gilfillan**[1]

[1]Laboratory of Allergic Diseases, National Institute of Allergy and Infectious Diseases, National Institutes of Health, Bethesda, MD, USA

[2]Laboratory of Molecular Immunology, National Heart, Lung, and Blood Institute, National Institutes of Health, Bethesda, MD, USA

Summary

Following antigen/IgE-mediated aggregation of high affinity IgE-receptors (FcεRI), mast cells (MCs) degranulate and release inflammatory mediators leading to the induction of allergic reactions including anaphylaxis. Migration of MCs to resident tissues and sites of inflammation is regulated by tissue chemotactic factors such as stem cell factor (SCF [KIT ligand]). Despite inducing similar early signaling events to antigen, chemotactic factors, including SCF, produce minimal degranulation in the absence of other stimuli. We therefore investigated whether processes regulating MC chemotaxis are rate limiting for MC mediator release. To investigate this issue, we disrupted actin polymerization, a requirement for MC chemotaxis, with latrunculin B and cytochalasin B, then examined chemotaxis and mediator release in human (hu)MCs induced by antigen or SCF. As expected, such disruption minimally affected early signaling pathways, but attenuated SCF-induced huMC chemotaxis. In contrast, SCF, in the absence of other stimuli, induced substantial degranulation in a concentration-dependent manner following actin disassembly. It also moderately enhanced antigen-mediated huMC degranulation which was further enhanced in the presence of SCF. These observations suggest that processes regulating cell migration limit MC degranulation as a consequence of cytoskeletal reorganization.

Keywords

chemotaxis; degranulation; F-actin; KIT; Mast Cell; SCF

Introduction

Mast cell (MC) activation, with the subsequent release of inflammatory mediators, is a central process in the initiation of allergic inflammation. Antigen-induced aggregation of the IgE-high affinity IgE receptor (FcεRI) complex is considered the principle mode of initiating the necessary signaling cascades for mediator release [1]. Nevertheless, other intrinsic, extrinsic, or physical stimuli can modulate antigen-dependent MC activation or, by themselves, induce MC mediator release in experimental models [2]. However, the extent to which these other stimuli contribute to MC-induced pathology in humans is not entirely clear.

**Current address and address for correspondence: Daniel Smrž, Institute of Immunology, 2nd Medical School and University Hospital Motol, Charles University, V Úvalu 84, 150 06 Praha 5, Czech Republic, EU, Fax: +420-22443-5962; daniel.smrz@lfmotol.cuni.cz.

Conflict of interests
The authors declare no financial or commercial conflict of interest.

MC infiltration is observed at sites of inflammation and is also associated with chronic allergic disease and bacterial and helminthic infections [3–6]. Stem cell factor (SCF), the ligand for the MC growth factor receptor, KIT, is a principle factor produced within tissues that can induce MC chemotaxis [7]. SCF is required for MC homeostasis [8], and can synergize with antigen to enhance MC degranulation and cytokine production [9, 10]. However, SCF induces minimal degranulation in the absence of other stimuli [9]. In contrast, antigen potently induces MC degranulation but is a much weaker stimulant of chemotaxis than SCF even though activated KIT and FcεRI initiate many of the same early signaling events in MCs [11]. These data suggest that, chemotaxis and degranulation may be inversely regulated such that distal processes that regulate chemotaxis may be rate limiting for degranulation.

One common distal feature of MC degranulation and chemotaxis is the requirement for cytoskeletal reorganization which occurs as a result of polymerized (filamentous; F)-actin de-polymerization/re-polymerization [12]. It is thought that F-actin de-polymerization facilitates granule extrusion from the cytosol during exocytosis [13–16] whereas, conversely, we [17] and others [18–21] have shown that actin polymerization is crucial for MC chemotaxis. We have, therefore, examined the possibility that the balance of these opposing actions may direct MC function with regards to the relative exclusivity of degranulation and chemotaxis of activated MCs.

Here we show that disruption of actin polymerization attenuated SCF-induced migration of human (hu)MCs whereas the ability of SCF to amplify antigen-mediated degranulation or to induce degranulation on its own was markedly enhanced. These data thus reveal that processes regulating F-actin dynamics, leading to cytoskeletal reorganization, dictate the outcome of the MC response to antigen and SCF, and furthermore suggest that actin polymerization during chemotaxis may be rate limiting for degranulation.

Results

Contrasting chemotaxis and degranulation in huMCs induced through FcεRI and KIT

We first compared the effects of FcεRI aggregation, induced by the addition of streptavidin (SA) to biotinylated human (hu)IgE-sensitized cells, and KIT activation, induced by the addition of SCF, on huMC degranulation and chemotaxis. As previously reported [10, 22, 23], FcεRI aggregation induced a dose-dependent increase in huMC degranulation, whereas KIT activation produced no evidence of degranulation (Fig. 1A). In contrast to degranulation and the slight chemotactic response observed in mouse bone marrow-derived MCs (BMMCs) [17], such FcεRI aggregation failed to evoke huMC chemotaxis whereas SCF-induced KIT activation markedly promoted this response (Fig. 1B). Thus, in huMCs and in the absence of other stimuli, the processes of MC degranulation and migration, as mediated via FcεRI and KIT, appear to be exclusive of each other.

F-actin content increases in both SA- or SCF-stimulated huMCs

F-actin de-polymerization/re-polymerization is a critical process in MC degranulation [13, 14, 18, 24]. In BMMCs, antigen induces rapid (0–2 minutes after activation) F-actin de-polymerization, followed by re-polymerization which often results in levels greater than that observed in non-stimulated cells [17, 18, 25]. In the rat basophilic leukemia cell line (RBL-2H3), the initial rapid de-polymerization is not observed, but a similar increase in total F-actin in the cells occurs in later phases of cell activation (5–30 min) [13, 24, 26]. It is thought that disruption of the F-actin barrier is essential to allow the granules to migrate through the cytosol and cytoplasmic membrane [27]. Conversely, actin polymerization has

been shown to be critical for MC chemotaxis [7]. We thus examined whether FcεRI aggregation (SA) and SCF affected the status of F-actin in huMCs in dissimilar ways.

In contrast to the noticeable reorganization of the F-actin ring formation observed in BMMCs activated with antigen [15], we observed minimal gross changes in the membrane ring structure in huMCs following challenge with either SA or SCF when examined qualitatively using confocal microscopy (Fig. 2A). Furthermore, we observed no discernible differences in the relative localization of cytosolic granules and F-actin, as assessed by MC tryptase and F-actin staining under these conditions (Fig. 2A).

Adopting a more quantitative approach, we examined F-actin by FACS analysis following phalloidin staining. We found that both SA and SCF stimulation resulted in a rapid and prolonged increase in F-actin content in the huMCs (Fig. 2B and C). This indicated that, although no discernible structural changes in F-actin assembly were perceived by confocal microscopy, as observed in other MC systems [27], both FcεRI- and SCF-mediated stimulation of huMCs was associated with F-actin assembly.

Disruption of actin polymerization in huMCs attenuates SCF-induced huMC chemotaxis

To investigate the relative roles of such actin polymerization in huMC chemotaxis and degranulation, we disrupted this process with latrunculin B [28], a macrolide compound that binds to monomeric actin, thus preventing its ability to polymerize [29]. As shown in Figure 3A, latrunculin B noticeably disrupted integrity of the F-actin ring in the huMCs, both in the resting cells and those challenged with SCF. Furthermore, latrunculin B-mediated F-actin disassembly was enhanced after SCF stimulation (Fig. 3B), thus indicating that both actin polymerization and depolymerization occurs simultaneously following SCF challenge.

The outcome of this disruption of F-actin organization on SCF-induced huMC chemotaxis was next examined. As predicted from previous studies [17, 20, 30], latrunculin B completely prevented the ability of huMC to migrate towards SCF (Fig. 4A). This was not due to an adverse effect on cell viability as determined by lack of any increase in annexin-positive cells under these experimental conditions (Fig. 4B). Therefore, these data confirm that disruption of F-actin assembly directly inhibits huMC migration.

Disruption of actin polymerization in huMCs has marginal effect on early SCF-induced signaling

To establish that the inhibition of huMC chemotaxis by prevention of actin polymerization was not a consequence of disruption of key signaling events, we next examined the ability of latrunculin B to inhibit the ability of SCF to initiate phospholipase (PL)Cγ and PI3K activation which are responsible for inducing the calcium signal known to regulate MC chemotaxis [7, 31]. To do this, we respectively examined the phosphorylation status of $PLC\gamma_1$ and $PLC\gamma_2$, and of the surrogate PI3K activation marker, protein kinase B (AKT), 2 min after addition of SCF. We also examined the phophorylation status of MAP kinases (ERK 1/2, JNK, and P38) which also contribute to this response [7]. As shown in Fig. 5A and Supporting Information Fig. 1A, SCF-induced signals leading to the calcium response were not inhibited under conditions that disrupt actin polymerization. If anything, there was a slight increase in $PLC\gamma_1$ phosphorylation. Also, latrunculin B treatment had little effect on the phosphorylation of the MAP kinases except for a modest, albeit significant, increase in p38 phosphorylation (Fig. 5B and Supporting Information Fig. 1B). A modest increase was also observed in the calcium signal in latrunculin B-treated cells (Fig. 5C) which was consistent with the small increase in $PLC\gamma_1$ phosphorylation. This increase however did not reach the levels or the rapidity as observed in response to SA (Fig. 5D). Latrunculin B is reported to induce a calcium signal by itself in B cells [32] but this was not apparent in

huMCs (data not shown). Overall, our data suggested that latrunculin minimally perturbed early signaling events in huMCs.

Disruption of F-actin assembly enables SCF to induce degranulation of huMCs

Although SCF does not induce degranulation by itself, as shown in Fig. 6A and reported elsewhere [22], SCF induces a concentration-dependent increase in huMC degranulation with a maximal release at 30 ng/ml SCF in the presence of a threshold concentration SA (1 ng/ml). Also and similar to observations with mouse BMMCs [15], antigen-stimulated degranulation of huMCs was enhanced by latrunculin B (Fig. 6B). Of particular note, however, substantial degranulation (~40% release) was evoked by SCF in the absence of SA following latrunculin B treatment even though SCF does not normally induce degranulation (Fig. 6C). Degranulation was further augmented by co-stimulation with SA in a manner consistent with the potentiation observed on co-stimulation in the absence of latrunculin B (Fig. 6C).

The remarkable ability of SCF to induce degranulation in latrunculin-treated cells was further investigated over its effective concentration range (0–100 ng/ml; [22]) by comparing the effects of latrunculin B with cytochalasin B, a compound that binds to F-actin and prevents its elongation [33]. The presence of either inhibitor revealed that SCF in the absence of SA produced significant degranulation in a concentration-dependent manner with maximal degranulation being observed at 30 ng/ml. The responses observed in the latrunculin B-treated cells (Fig. 6D) exceeded those achieved with a threshold concentration of SA (as in Fig. 6A) and approached those obtained following optimal SA challenge (as in Fig. 6B). Treatment with cytochalasin B, which inhibits association and dissociation of actin subunits at the barbed ends of F-actin [33], also allowed SCF to induce degranulation, albeit to a lesser extent than latrunculin B (Fig. 6E). Since cytochalasin B may also retard disassembly of actin filaments, this may account for its reduced efficacy in promoting degranulation as compared with that of lantrunculin B if disassembly is an essential process in degranulation. Taken together, these data demonstrate that, regardless of the mechanism which the F-actin reorganization is attenuated, an inefficient F-actin reorganization relieves the block that prevents SCF from initiating degranulation in huMCs.

Disassembly of F-actin in huMCs potentiates the production of IL-8 by SCF

In addition to degranulation, activated MCs also generate a suite of cytokines and chemokines. Although SCF fails to induce degranulation, it can stimulate production of specific cytokines and chemokines by itself and this production is greatly enhanced in combination with antigen [9]. Hence, we examined whether disassembly of F-actin would also enhance cytokine release in response to SCF, either alone or in combination with antigen. As shown in Fig. 7, SCF alone caused no or minimal production of GM-CSF, MCP-1, and IL-8 but among these, only IL-8 production was markedly potentiated by latrunculin B treatment (Fig. 7A and C). Cell viability was unaffected by latrunculin B (Fig. 7D).

Examination of the activation state of transcription factors that drive cytokine production in mast cells revealed that SCF, in the absence or presence of latrunculin B, caused little or no activating phosphorylations of NFκB and NFAT by 30 min (data not shown). However, by 30 min (Fig. 7E–F), SCF stimulation had resulted in significant increases in levels of c-Jun and of phosphorylated c-Jun which were enhanced in latrunculin B-treated cells. The c-Jun gene is rapidly inducible by antigen [34], and apparently by SCF (this report), and c-Jun is a component of the activator protein complex, AP1, which is known to regulate IL-8 gene transcription [35]. How actin disassembly might promote induction of c-Jun is unclear at present.

Taken together these data reveal that by disrupting a critical process required for MC chemotaxis, actin polymerization, SCF acquires the ability to induce degranulation and an increase in the production of IL-8 but not of other cytokines examined.

Discussion

MCs are multifunctional cells whose diverse responses can be finely tuned by the concurrent or independent engagement of specific classes of cell surface receptors that may favor one type of response over others as for example chemotaxis over degranulation or cytokine production. The signaling pathways linking these receptors to their own particular responses have been described in detail [36] and it is clear that these pathways share common features, especially at the early stages of signaling. For example, although KIT, FcεRI, G protein-coupled receptors and Toll-like receptors (TLRs) mediate quite divergent responses, they all have the ability to activate PI3K and MAP kinases, and, with the exception of TLRs, induce a calcium signal [36–38]. Nevertheless, further studies are needed as to how these different classes of receptors can promote one particular response over another. In this study, we have investigated one aspect, namely the mutually exclusive abilities of FcεRI and KIT to induce respectively degranulation and chemotaxis in huMCs. We propose that such selectivity may be a consequence of a distal rate limiting process which, in the example described in this study, is associated with cytoskelatal rearrangement linked to actin polymerization.

Our current and previous studies [9, 23] indicate that, in the absence of other stimuli, huMCs have limited capacity to degranulate in response to SCF and to migrate following FcεRI aggregation. This observation differs from previous studies with rodent MCs [7, 39], including our own [17], in which FcεRI aggregation can induce chemotaxis but to a much lesser extent than SCF. The reason for this difference is unclear but, as with certain other responses [40], this would indicate that mouse MC biology may not reflect that of huMCs. Nevertheless, the data from both species point to differential regulation of MC degranulation and chemotaxis by antigen and SCF respectively.

To identify steps that limit degranulation while permitting chemotaxis in SCF-stimulated cells and the converse situation for antigen, we focused on actin polymerization/depolymerization since cytoskeletal reorganization is a key process in granule extrusion [14,41] and a driving force for cell migration [27,42]. Studies in mouse BMMCs suggest that extensive actin depolymerization is required for degranulation [15, 17]. However, we observed no F-actin rearrangement in huMCs in response to either SCF or following FcεRI cross-linking (Fig. 2) as has been reported for antigen-stimulated RBL-2H3 cells [13, 24, 26]. It is possible that the cycle of de-polymerization and re-polymerization occurs more rapidly in huMCs than in BMMCs and is complete before our 2 minute observation time-point. In addition and more likely, F-actin remodeling may be highly localized in huMCs such that actin de-polymerization occurs at some sites while re-polymerization occurs at other sites within individual cells. Regardless, it is apparent that extensive actin-remodeling takes place because of the increased SCF-induced depolymerization of F-actin in lantrunculin B-treated huMCs (Fig. 3) and that this actin-remodeling is required for huMC chemotaxis [20, 21, 26].

The ability to latrunculin B to dissociate the chemotactic from degranulation response to SCF without affecting early signaling events, allowed us to conclude that the mechanics of F-actin assembly/disassembly that are required for chemotaxis differ from and suppress those required for degranulation. The data also suggest that SCF simultaneously generates signals for chemotaxis and degranulation but those for chemotaxis normally predominate in huMCs, presumably at the level of F-actin remodeling. This conclusion was supported by the inability of SCF to induce degranulation concurrently with chemotaxis and by the switch

to degranulation instead of chemotaxis following disassembly of F-actin with latrunculin B. Too little is known about the differences between chemotaxis and degranulation in actin remodeling or the exact interactions with actin-regulatory proteins, to know how this switch to degranulation occurs. It is known that oscillations in F-actin assembly and cytosolic Ca^{2+} are tightly coupled in a latrunculin B-sensitive manner [43] and that the oscillations in calcium ions coincide with oscillatory bursts in degranulation [44] in antigen-stimulated RBL-2H3 MCs. However, comparable studies have not been conducted with SCF and, in particular, how these dynamics are altered by the combination of antigen and SCF.

Of note, SCF-mediated degranulation in the presence of latrunculin B occurred without compromised cell viability and within the normal concentration range used for SCF-mediated responses (i.e. 0–100 ng/ml). Of note, this response reached the magnitude of that observed with an optimal concentration of SA. Also, consistent with recent findings of potential links between cytoskeletal reorganization and cytokine release [45], SCF-induced IL-8 release was also enhanced following lantrunculin B-induced F-actin disassembly possibly through enhanced induction of c-Jun.

In summary, in this study we have described how a component of cytoskeletal rearrangement during SCF-mediated chemotaxis, namely F-actin assembly, limits degranulation, presumably due to differences in the type of F-actin remodeling required for chemotaxis and degranulation. The biological implications for our observations are three-fold. Firstly, the studies with latrunculin B indicate that F-actin assembly is critical for chemotaxis but not degranulation where disassembly may be the preeminent requirement and that SCF can generate signals for either process. Secondly, it could be assumed that it would be detrimental for MCs to degranulate, and thus become refractory to further stimulation during migration, prior to residing in their target tissues. As such, SCF and similar chemotactic agents would limit the capacity of MCs to degranulate while generating the required signals for chemotaxis. Lastly, migration to other tissues during innate and acquired defensive reactions which result in the generation and localized release of inflammatory mediators would be inefficient and undesirable. Whether disruption of such processes exists in disease states is unknown. However, if they were to occur, the consequences for progression of MC-driven disease would be profound.

Materials and Methods

Primary huMC culture

$CD34^+$ peripheral blood progenitors were isolated from healthy donors and used to prepare huMCs as described [46]. The donors provided an informed consent, and cells were obtained under a protocol (NCT00001756) approved by the National Institutes of Health Internal Review Board.

Antibodies and reagents

The protein-specific antibodies were: MC tryptase (Abcam, Cambridge, MA), β-actin (Sigma-Aldrich, St. Louis, MO; Cell Signaling Technology, Beverley, MA), fluorophore-conjugated antibodies (Jackson ImmunoResearch Laboratories, Inc., West Grove, PA), horseradish peroxidase-conjugated rabbit IgG (Amersham Biosciences, Piscataway, NJ), mouse IgG Fc-specific antibody (Sigma-Aldrich), and human myeloma IgE (Calbiochem, La Jolla, CA) biotinylated by the NIAID Core Facility. The phosphoprotein-specific antibodies to: KIT^{Y721} and $PLC\gamma_1{}^{Tyr783}$ (Invitrogen, Carlsbad,CA), $PLC\gamma_2{}^{Tyr759}$, AKT^{Thr308}, $ERK1/2^{Thr202/Tyr204}$, $JNK^{Thr183/Tyr185}$, $P38^{Thr180/Tyr182}$, $NF\kappa B^{Ser356}$, $c\text{-}Jun^{Ser63}$, c-Jun (Cell Signaling Technology, Beverley, MA) and $NFAT^{Tyr339}$ (Santa Cruz

Biotechnology, Santa Cruz, CA) Other reagents: donkey serum (Santa Cruz Biotechnology), FITC- or TRITC-conjugated phalloidin, latrunculin B and cytochalasin B (Sigma-Aldrich).

Cell activation

HuMCs were, or were not, sensitized with bio-huIgE; 100 ng/ml [47] and starved in cytokine-free media overnight. FcεRI aggregation was subsequently achieved by cross-linking the bio-huIgE with SA. For immunoblotting, degranulation, flow cytometry, and confocal microscopy studies, the cells were harvested and then activated as described [48]. For cytokine release studies, the cells were washed with cytokine-free media and stimulated by adding an equal amount of 2× stimulant in cytokine-free media and the cells were further incubated at 37 °C / 5 % CO_2 for the time period indicated.

Degranulation, cytokine production

Degranulation was determined after 30 min activation as a percentage of β-hexosaminidase released into supernantant [49]. Cytokine production was determined after 6 h activation and calculated as a concentration of cytokines released by 1.0×10^6 cells/ml cells into supernatant using Quantikine ELISA kits (R&D Systems, Minneapolis, MN).

Immunoblotting, flow cytometry and calcium measurement

Lysates of the activated cells were prepared and analyzed by immunoblotting as described [48]. Annexin V/PI staining was performed as described [50]. To label F-actin, the activated cells were fixed with [4% (w/v) paraformaldehyde, 5 mM EDTA, 5 mM EGTA, PBS] for 30 min, washed with PBS then permeabilized with [0.1 % (v/v) Triton-X100, 5 % (w/v) BSA, 2 mM EGTA, PBS] for 5 min. The cells were washed with PBS and quenched with [5 % (w/v) BSA, 2 mM EGTA, PBS] for 30 min then incubated with 1 μg/ml phalloidin-TRITC in [5 % (w/v) BSA, 2 mM EGTA, PBS] for 1 h and washed with [0.5 % (w/v) BSA, 0.2 mM EGTA, PBS] followed by PBS. The stained cells were analyzed by flow cytometry using FACSCalibur with CellQuest 3.3 software (BD Biosciences), and the acquired data analyzed by FlowJo 7.6 software (TreeStar). The intact cells (Supporting Information Fig. 2A) were used for evaluation in the phalloidin-FITC staining assays. An additional gating used in the evaluation is indicated in the figures. The calcium measurement was performed as described [51].

Migration assay

Migration assays were performed in Transwell® permeable supports with 8.0 μm pore size membrane in a 24-well plate (Costar®) (Corning, Corning, NY). Cells were transferred into cytokine-free media ($0.5–4 \times 10^6$), then mixed (1:1) with the cytokine-free media with or without the indicated inhibitor. One hundred μl of the suspension was then transferred to the upper chamber and this chamber placed over the bottom chamber containing 600 μl cytokine-free media with or without the inhibitor. After 30 min incubation at 37 °C / 5 % CO_2, the upper chambers were replaced over the bottom chambers containing 600 μl cytokine-free media with or without the inhibitor and containing, or not, SCF (10 ng/ml). After 4 h incubation at 37 °C / 5 % CO_2, the upper chambers were removed, the migrated cells in the bottom chamber collected and their numbers determined. A post-assay viability of the cells in the upper chamber was determined by annexin V/PI staining and flow cytometry as described above. The PI/Annexin V positive cell populations were considered as dead cells (Supporting Information Fig. 2B).

Confocal microscopy

Cell activation was stopped by adding an equal amount of (40 mM EDTA, 40mM EGTA, PBS) and the cells were transferred onto poly-lysine (100 μg/ml) coated slides positioned in

a 24-well plate. After 5 min, the cells were fixed with 1 ml of (4% (w/v) paraformaldehyde, 5 mM EDTA, 5 mM EGTA, PBS) for 30 min. The fixed cells were washed with PBS and permeabilized with (0.1 % (v/v) Triton-X100, 5 % (w/v) BSA, 2 mM EGTA, PBS) for 5 min. The cells were washed with PBS and quenched with (5 % (w/v) BSA, 2 mM EGTA, PBS) for 30 min. The cells were then incubated with 5 μg/ml MC mouse tryptase-specific antibody and 1 μg/ml phalloidin-TRITC in (5 % (w/v) BSA, 2 mM EGTA, PBS supplemented with 200 × diluted donkey serum) for 1 h. The cells were washed with PBS and (5 % (w/v) BSA, 2 mM EGTA, PBS) and then incubated with 5–10 μg/ml donkey mouse IgG-specific Alexa488-conjugared secondary antibody in (5 % (w/v) BSA, 2 mM EGTA, PBS supplemented with 200 × diluted donkey serum) for 1 h. The cells were washed with (5 % (w/v) BSA, 2 mM EGTA, PBS), then PBS. The cells were stained with DAPI (2 μg/ml) for 10–20 min, washed with PBS then mounted on support slides using Prolong® Gold anti-fade reagent (Invitrogen). The images were acquired on Leica SP5 confocal microscope (Leica Microsystems, Exton, PA) using 63× oil immersion objective with numerical aperture 1.4. The acquired images were deconvolved with Huygens Essential software (Scientific Volume Imaging BV, Hilversum, The Netherlands) and processed with Imaris software (Bitplane AG, Zurich, Switzerland).

Statistical analysis

Means and SEM were computed from the number of individual experiments indicated where each individual experiment is defined as that conducted on cells derived from different individual donors. Where multiple experiments were conducted using the same donor, these results were averaged prior to inclusion in the final analysis as a single replicate. Unpaired Student *t* test was used to determine the statistical significance of differences between groups. Data were considered significant when $P<0.05$.

Supplementary Material

Refer to Web version on PubMed Central for supplementary material.

Acknowledgments

Research in the authors' laboratories was supported by funding from the Intramural Research programs within NIAID (D.S., D.D.M. and A.M.G.) and NHLBI (M.A.B). We would like to thank Biological Imaging Facility (RTB/NIAID/NIH) for technical support in confocal image acquisition including Juraj Kabat for assistance in image post processing and analysis.

Abbreviations

BMMC	bone marrow-derived mast cell
F-actin	filamentous actin
FcεRI	high affinity IgE receptor
huMC	human mast cell
MC	mast cell
RBL 2H3	rat basophilic leukemia 2H3 mast cell line
SA	streptavidin
SCF	stem cell factor

References

1. Kraft S, Kinet JP. New developments in FcεRI regulation, function and inhibition. Nat. Rev. Immunol. 2007; 7:365–378. [PubMed: 17438574]
2. Gilfillan AM, Beaven MA. Regulation of mast cell responses in health and disease. Crit. Rev. Immuno.l. 2011; 31:475–529.
3. Metcalfe DD, Baram D, Mekori YA. Mast cells. Physiol. Rev. 1997; 77:1033–1079. [PubMed: 9354811]
4. Metz M, Grimbaldeston MA, Nakae S, Piliponsky AM, Tsai M, Galli SJ. Mast cells in the promotion and limitation of chronic inflammation. Immunol. Rev. 2007; 217:304–328. [PubMed: 17498068]
5. Madden KB, Urban JF Jr, Ziltener HJ, Schrader JW, Finkelman FD, Katona IM. Antibodies to IL-3 and IL-4 suppress helminth-induced intestinal mastocytosis. J. Immunol. 1991; 147:1387–1391. [PubMed: 1869831]
6. Echtenacher B, Männel DN, Hültner L. Critical protective role of mast cells in a model of acute septic peritonitis. Nature. 1996; 381:75–77. [PubMed: 8609992]
7. Halova I, Draberova L, Draber P. Mast cell chemotaxis - chemoattractants and signaling pathways. Front. Immunol. 2012; 3:119. [PubMed: 22654878]
8. Okayama Y, Kawakami T. Development, migration, and survival of mast cells. Immunol. Res. 2006; 34:97–115. [PubMed: 16760571]
9. Hundley TR, Gilfillan AM, Tkaczyk C, Andrade MV, Metcalfe DD, Beaven MA. Kit and FcεRI mediate unique and convergent signals for release of inflammatory mediators from human mast cells. Blood. 2004; 104:2410–2417. [PubMed: 15217825]
10. Nagasaka A, Matsue H, Matsushima H, Aoki R, Nakamura Y, Kambe N, Kon S, et al. Osteopontin is produced by mast cells and affects IgE-mediated degranulation and migration of mast cells. Eur. J. Immunol. 2008; 38:489–499. [PubMed: 18200503]
11. Gilfillan AM, Rivera J. The tyrosine kinase network regulating mast cell activation. Immunol. Rev. 2009; 228:149–169. [PubMed: 19290926]
12. Stricker J, Falzone T, Gardel ML. Mechanics of the F-actin cytoskeleton. J. Biomech. 2010; 43:9–14. [PubMed: 19913792]
13. Tolarová H, Dráberová L, Heneberg P, Dráber P. Involvement of filamentous actin in setting the threshold for degranulation in mast cells. Eur. J. Immunol. 2004; 34:1627–1636. [PubMed: 15162432]
14. Pendleton A, Koffer A. Effects of latrunculin reveal requirements for the actin cytoskeleton during secretion from mast cells. Cell Motil. Cytoskeleton. 2001; 48:37–51. [PubMed: 11124709]
15. Nishida K, Yamasaki S, Ito Y, Kabu K, Hattori K, Tezuka T, Nishizumi H, et al. FcεRI-mediated mast cell degranulation requires calcium-independent microtubule-dependent translocation of granules to the plasma membrane. J. Cell. Biol. 2005; 170:115–126. [PubMed: 15998803]
16. Deng Z, Zink T, Chen HY, Walters D, Liu FT, Liu GY. Impact of actin rearrangement and degranulation on the membrane structure of primary mast cells: a combined atomic force and laser scanning confocal microscopy investigation. Biophys. J. 2009; 96:1629–1639. [PubMed: 19217878]
17. Kuehn HS, Rådinger M, Brown JM, Ali K, Vanhaesebroeck B, Beaven MA, Metcalfe DD, et al. Btk-dependent Rac activation and actin rearrangement following FcεRI aggregation promotes enhanced chemotactic responses of mast cells. J. Cell. Sci. 2010; 123:2576–2585. [PubMed: 20587594]
18. Tůmová M, Koffer A, Šimíček M, Dráberová L, Dráber P. The transmembrane adaptor protein NTAL signals to mast cell cytoskeleton via the small GTPase Rho. Eur. J. Immunol. 2010; 40:3235–3245. [PubMed: 21061444]
19. Liu L, Chen L, Chung J, Huang S. Rapamycin inhibits F-actin reorganization and phosphorylation of focal adhesion proteins. Oncogene. 2008; 27:4998–5010. [PubMed: 18504440]
20. Gebhardt T, Gerhard R, Bedoui S, Erpenbeck VJ, Hoffmann MW, Manns MP, Bischoff SC. β2-Adrenoceptor-mediated suppression of human intestinal mast cell functions is caused by

disruption of filamentous actin dynamics. Eur. J. Immunol. 2005; 35:1124–1132. [PubMed: 15756641]

21. Shimizu T, Owsianik G, Freichel M, Flockerzi V, Nilius B, Vennekens R. TRPM4 regulates migration of mast cells in mice. Cell Calcium. 2009; 45:226–232. [PubMed: 19046767]
22. Tkaczyk C, Horejsi V, Iwaki S, Draber P, Samelson LE, Satterthwaite AB, Nahm DH, et al. NTAL phosphorylation is a pivotal link between the signaling cascades leading to human mast cell degranulation following Kit activation and FcεRI aggregation. Blood. 2004; 104:207–214. [PubMed: 15010370]
23. Iwaki S, Tkaczyk C, Satterthwaite AB, Halcomb K, Beaven MA, Metcalfe DD, Gilfillan AM. Btk plays a crucial role in the amplification of FcεRI-mediated mast cell activation by kit. J. Biol. Chem. 2005; 280:40261–40270. [PubMed: 16176929]
24. Frigeri L, Apgar JR. The role of actin microfilaments in the down-regulation of the degranulation response in RBL-2H3 mast cells. J. Immunol. 1999; 162:2243–2250. [PubMed: 9973500]
25. Sasaki J, Sasaki T, Yamazaki M, Matsuoka K, Taya C, Shitara H, Takasuga S, et al. Regulation of anaphylactic responses by phosphatidylinositol phosphate kinase type I α. J. Exp. Med. 2005; 201:859–870. [PubMed: 15767368]
26. Lee J, Veatch SL, Baird B, Holowka D. Molecular mechanisms of spontaneous and directed mast cell motility. J. Leukoc. Biol. 2012; 92:1029–1041. [PubMed: 22859829]
27. Draber P, Sulimenko V, Draberova E. Cytoskeleton in mast cell signaling. Front. Immunol. 2012; 3:130. [PubMed: 22654883]
28. Spector I, Shochet NR, Kashman Y, Groweiss A. Latrunculins: novel marine toxins that disrupt microfilament organization in cultured cells. Science. 1983; 219:493–495. [PubMed: 6681676]
29. Coué M, Brenner SL, Spector I, Korn ED. Inhibition of actin polymerization by latrunculin A. FEBS Lett. 1987; 213:316–318. [PubMed: 3556584]
30. Kuehn HS, Jung MY, Beaven MA, Metcalfe DD, Gilfillan AM. Prostaglandin E2 activates and utilizes mTORC2 as a central signaling locus for the regulation of mast cell chemotaxis and mediator release. J. Biol. Chem. 2011; 286:391–402. [PubMed: 20980255]
31. Holowka D, Calloway N, Cohen R, Gadi D, Lee J, Smith NL, Baird B. Roles for Ca^{2+} mobilization and its regulation in mast cell functions. Front. Immunol. 2012; 3:104. [PubMed: 22586429]
32. Treanor B, Depoil D, Gonzalez-Granja A, Barral P, Weber M, Dushek O, Bruckbauer A, et al. The membrane skeleton controls diffusion dynamics and signaling through the B cell receptor. Immunity. 2010; 32:187–199. [PubMed: 20171124]
33. Cooper JA. Effects of cytochalasin and phalloidin on actin. J. Cell Biol. 1987; 105:1473–1478. [PubMed: 3312229]
34. Razin E, Szallasi Z, Kazanietz MG, Blumberg PM, Rivera J. Protein kinases C-β and C-ε link the mast cell high-affinity receptor for IgE to the expression of c-*fos* and c-*jun*. Proc. Natl. Acad. Sci. U S A. 1994; 91:7722–7726. [PubMed: 8052650]
35. Holtmann H, Winzen R, Holland P, Eickemeier S, Hoffmann E, Wallach D, Malinin NL, et al. Induction of interleukin-8 synthesis integrates effects on transcription and mRNA degradation from at least three different cytokine- or stress-activated signal transduction pathways. Mol. Cell Biol. 1999; 19:6742–6753. [PubMed: 10490613]
36. Gilfillan AM, Tkaczyk C. Integrated signalling pathways for mast-cell activation. Nat. Rev. Immunol. 2006; 6:218–230. [PubMed: 16470226]
37. Rivera J, Gilfillan AM. Molecular regulation of mast cell activation. J. Allergy Clin. Immunol. 2006; 117:1214–1225. [PubMed: 16750977]
38. Qiao H, Andrade MV, Lisboa FA, Morgan K, Beaven MA. FcεR1 and toll-like receptors mediate synergistic signals to markedly augment production of inflammatory cytokines in murine mast cells. Blood. 2006; 107:610–618. [PubMed: 16174756]
39. Kitaura J, Eto K, Kinoshita T, Kawakami Y, Leitges M, Lowell CA, Kawakami T. Regulation of highly cytokinergic IgE-induced mast cell adhesion by Src, Syk, Tec, and protein kinase C family kinases. J. Immunol. 2005; 174:4495–4504. [PubMed: 15814670]
40. Bischoff SC. Role of mast cells in allergic and non-allergic immune responses: comparison of human and murine data. Nat. Rev. Immunol. 2007; 7:93–104. [PubMed: 17259966]

41. Malacombe M, Bader MF, Gasman S. Exocytosis in neuroendocrine cells: new tasks for actin. Biochim. Biophys. Acta. 2006; 1763:1175–1183. [PubMed: 17034880]
42. Rottner K, Stradal TE. Actin dynamics and turnover in cell motility. Curr. Opin. Cell Biol. 2011; 23:569–578. [PubMed: 21807492]
43. Wu M, Wu X, De Camilli P. Calcium oscillations-coupled conversion of actin travelling waves to standing oscillations. Proc. Natl. Acad. Sci. U S A. 2013; 110:1339–1344. [PubMed: 23297209]
44. Cohen R, Corwith K, Holowka D, Baird B. Spatiotemporal resolution of mast cell granule exocytosis reveals correlation with Ca^{2+} wave initiation. J. Cell Sci. 2012; 125:2986–2994. [PubMed: 22393234]
45. Ito T, Smrž D, Jung MY, Bandara G, Desai A, Smržová Š, Kuehn HS, et al. Stem cell factor programs the mast cell activation phenotype. J. Immunol. 2012; 188:5428–5437. [PubMed: 22529299]
46. Kirshenbaum AS, Goff JP, Semere T, Foster B, Scott LM, Metcalfe DD. Demonstration that human mast cells arise from a progenitor cell population that is $CD34^{+}$, c-kit^{+}, and expresses aminopeptidase N (CD13). Blood. 1999; 94:2333–2342. [PubMed: 10498605]
47. Kuehn HS, Rådinger M, Gilfillan AM. Measuring mast cell mediator release. Curr. Protoc. Immunol. 2010; Chapter 7(Unit7):38. [PubMed: 21053305]
48. Smrž D, Iwaki S, McVicar DW, Metcalfe DD, Gilfillan AM. TLR-mediated signaling pathways circumvent the requirement for DAP12 in mast cells for the induction of inflammatory mediator release. Eur. J. Immunol. 2010; 40:3557–3569. [PubMed: 21108475]
49. Choi OH, Lee JH, Kassessinoff T, Cunha-Melo JR, Jones SVP, Beaven MA. Antigen and carbachol mobilize calcium by similar mechanisms in a transfected mast cell line (RBL-2H3 cells) that expresses m1 muscarinic receptors. J. Immunol. 1993; 151:5586–5595. [PubMed: 8228248]
50. Smrž D, Dráberová L, Dráber P. Non-apoptotic phosphatidylserine externalization induced by engagement of glycosylphosphatidylinositol-anchored proteins. J. Biol. Chem. 2007; 282:10487–10497. [PubMed: 17284440]
51. Tkaczyk C, Beaven MA, Brachman SM, Metcalfe DD, Gilfillan AM. The phospholipase $C\gamma_1$-dependent pathway of FcεRI-mediated mast cell activation is regulated independently of phosphatidylinositol 3-kinase. J. Biol. Chem. 2003; 278:48474–48484. [PubMed: 13129935]

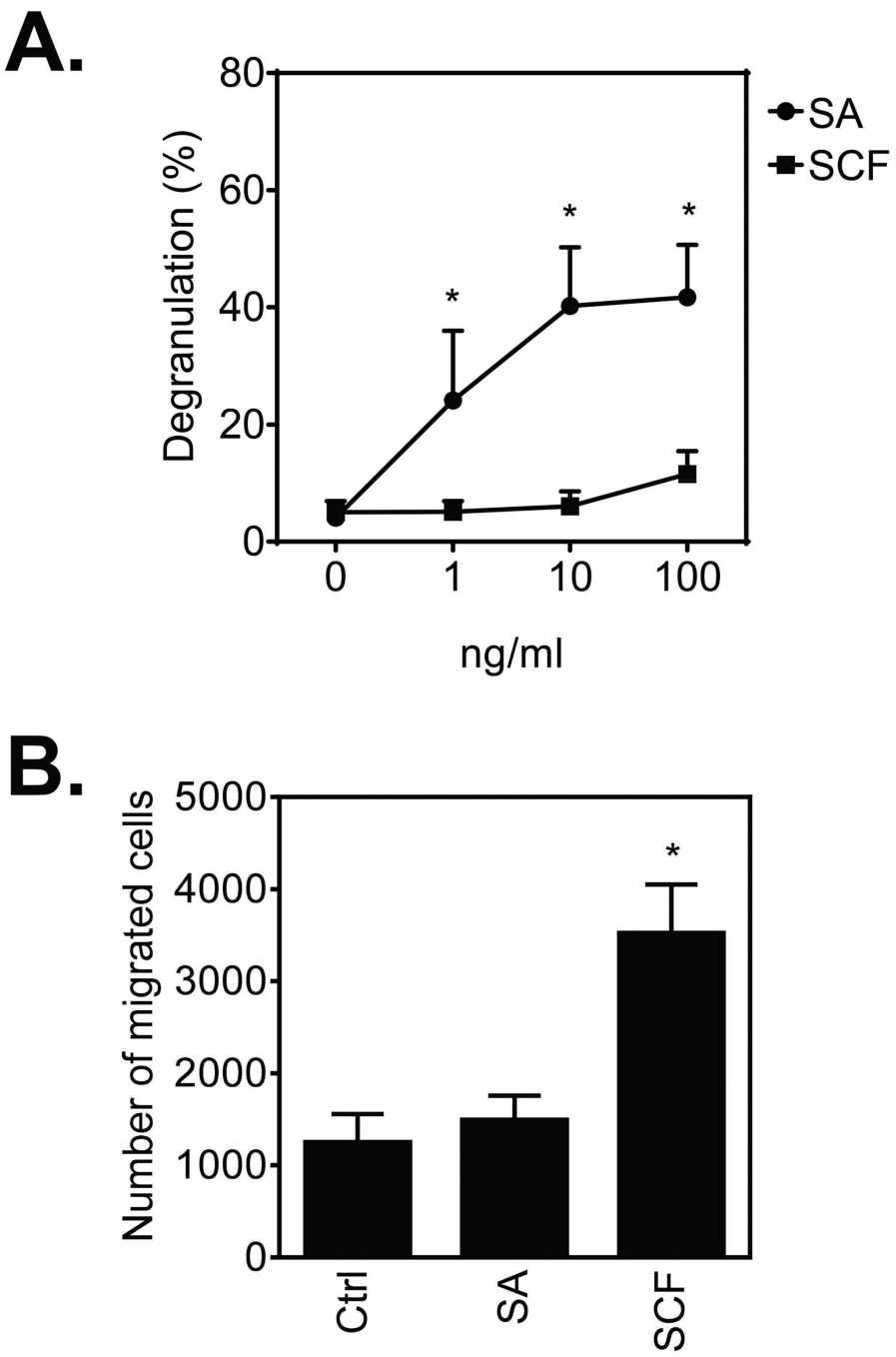

Figure 1.

Differential regulation of huMC degranulation and migration by FcεRI and KIT. (**A**) Sensitized (bio-huIgE; 100 ng/ml) and cytokine-starved (overnight) huMCs were activated with SA or SCF (0–100 ng/ml) for 30 min and degranulation was determined. (**B**) Sensitized and starved huMCs were transferred into cytokine-free media and the number of cells migrating through a 8.0 μm pore membrane towards vehicle (Ctrl; control), SA (10 ng/ml) or SCF (10 ng/ml) after 4 h was determined. (**A, B**) Data are shown as mean + SEM of n=3 individual donors and *P<0.05, Student's t-test, between SA- and SCF-stimulation (**A**), or control (Ctrl) and SA- or SCF-induced chemotaxis (**B**).

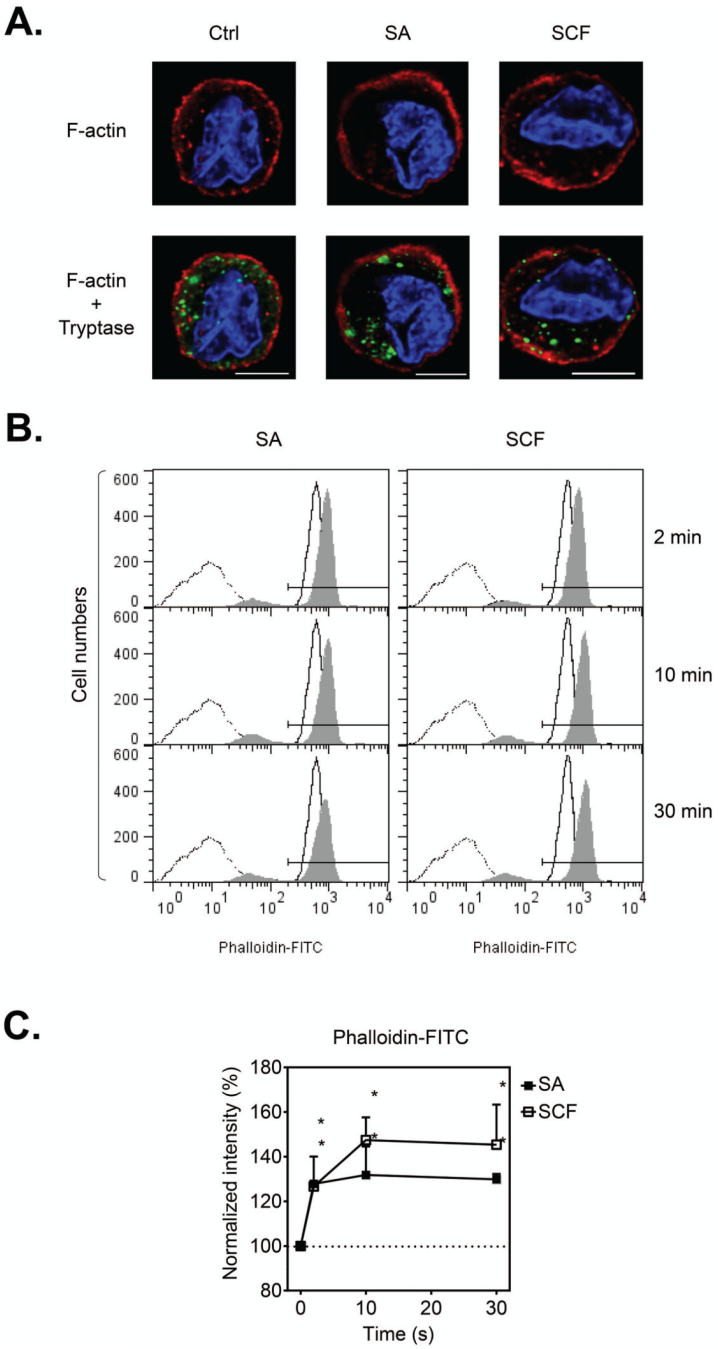

Figure 2.

F-actin content in huMCs following FcεRI aggregation or KIT activation. (**A**) Sensitized (bio-huIgE; 100 ng/ml) and cytokine-starved (overnight) huMCs were activated with vehicle alone (Ctrl), SA (100 ng/ml), or SCF (100 ng/ml) for 2 min. Immobilized, fixed and permeabilized cells were stained for F-actin (phalloidin-TRITC; red), MC tryptase (green), and nucleus (DAPI; blue), The cells were then analyzed by confocal microscopy and acquired images deconvolved. Scale bars represent 5 μm. (**B**) Sensitized and starved huMCs were activated with vehicle alone (solid line histogram), or SA or SCF (100 ng/ml; filled histogram) for the indicated time periods. Fixed and permeabilized cells were stained for F-

actin with phalloidin-FITC and analyzed by flow cytometry. Unstained and unstimulated cells (dotted line) were used as a negative control. (**A, B**) Data shown are representative of data obtained from 3 individual donors. (**C**) The fluorescence of phalloidin-FITC positive cells in (**B**) (the gate indicated) was normalized and evaluated, and shown as mean + SEM of n=3 donors. *P<0.05, Student's t-test.

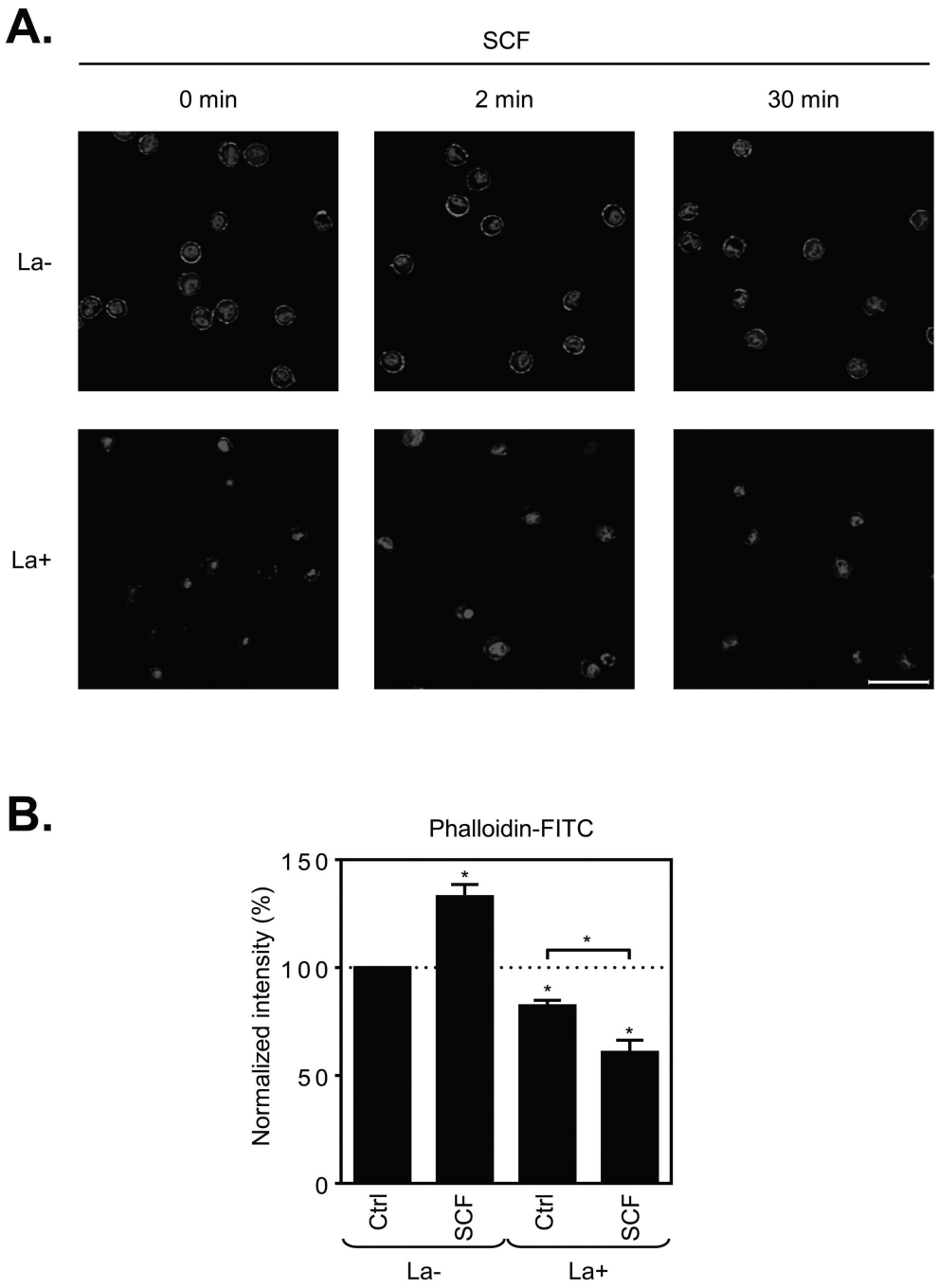

Figure 3.

Inhibition of actin polymerization by latrunculin B in resting and SCF-stimulated huMCs. (**A**) Non-sensitized and cytokine-starved huMCs were pre-treated (La+), or not (La−), with latrunculin B (1 μM) for 20 min and then activated with SCF (100 ng/ml) for the times indicated. Immobilized, fixed and permeabilized cells were stained for F-actin (phalloidin-TRITC; red) and nucleus (DAPI; blue), and then analyzed by confocal microscopy. Scale bars represent 20 μm. Data shown are representative of images analyzed from 3 donors. (**B**) Non-sensitized and starved huMCs were pre-treated (La+), or not (La−), with latrunculin B (1 μM) for 20 min and then activated with vehicle alone (Ctrl) or SCF (100 ng/ml) for 2 min.

Fixed and permeabilized cells were stained for F-actin with phalloidin-FITC and analyzed by flow cytometry. Unstained and unstimulated cells were used as a negative control. The fluorescence of phalloidin-FITC positive cells (gated as in Fig. 1B) was normalized and evaluated, and shown as mean + SEM of n=3 individual donors. *P<0.05, Student's t-test.

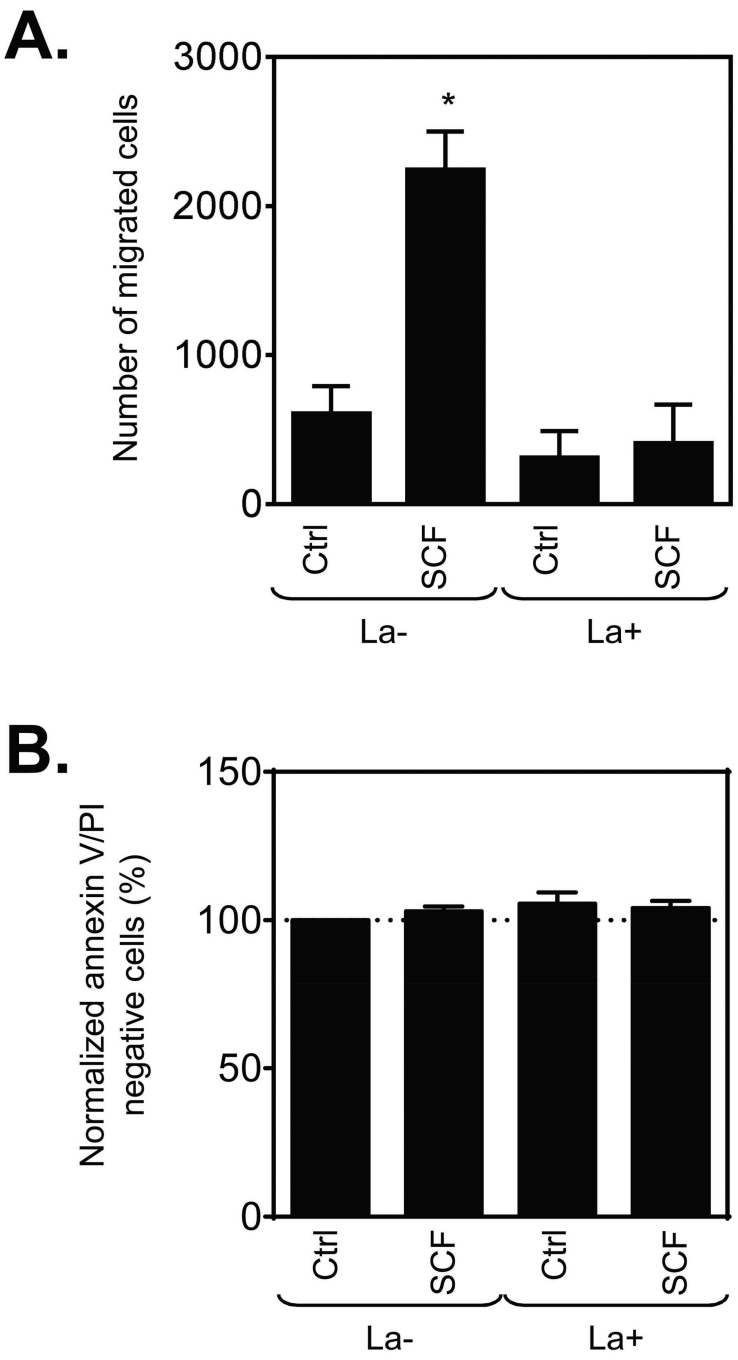

Figure 4.

Effect of disrupted actin polymerization on SCF-induced huMC chemotaxis. (**A**) Sensitized (bio-huIgE; 100 ng/ml) and cytokine-starved huMCs were transferred into cytokine-free media with or without latrunculin B (1 μM) and incubated at 37°C for 30 min. Then the number of cells migrating through a 8.0 μm pore membrane towards vehicle (Ctrl; chemokinesis) or SCF (10 ng/ml) in the presence or absence of latrunculin B (1 μM) after 4 h was determined. (**B**) Post-assay viability of cells in (**A**) was determined by annexin V/PI staining and flow cytometry, and normalized data were evaluated. (**A, B**) Data are shown as mean + SEM of n=3 individual donors. *P<0.05, Student's t-test, between chemokinesis

(Ctrl) in the presence (La+) or absence (La−) of latrunculin B, or chemokinesis (Ctrl) and SCF-induced chemotaxis.

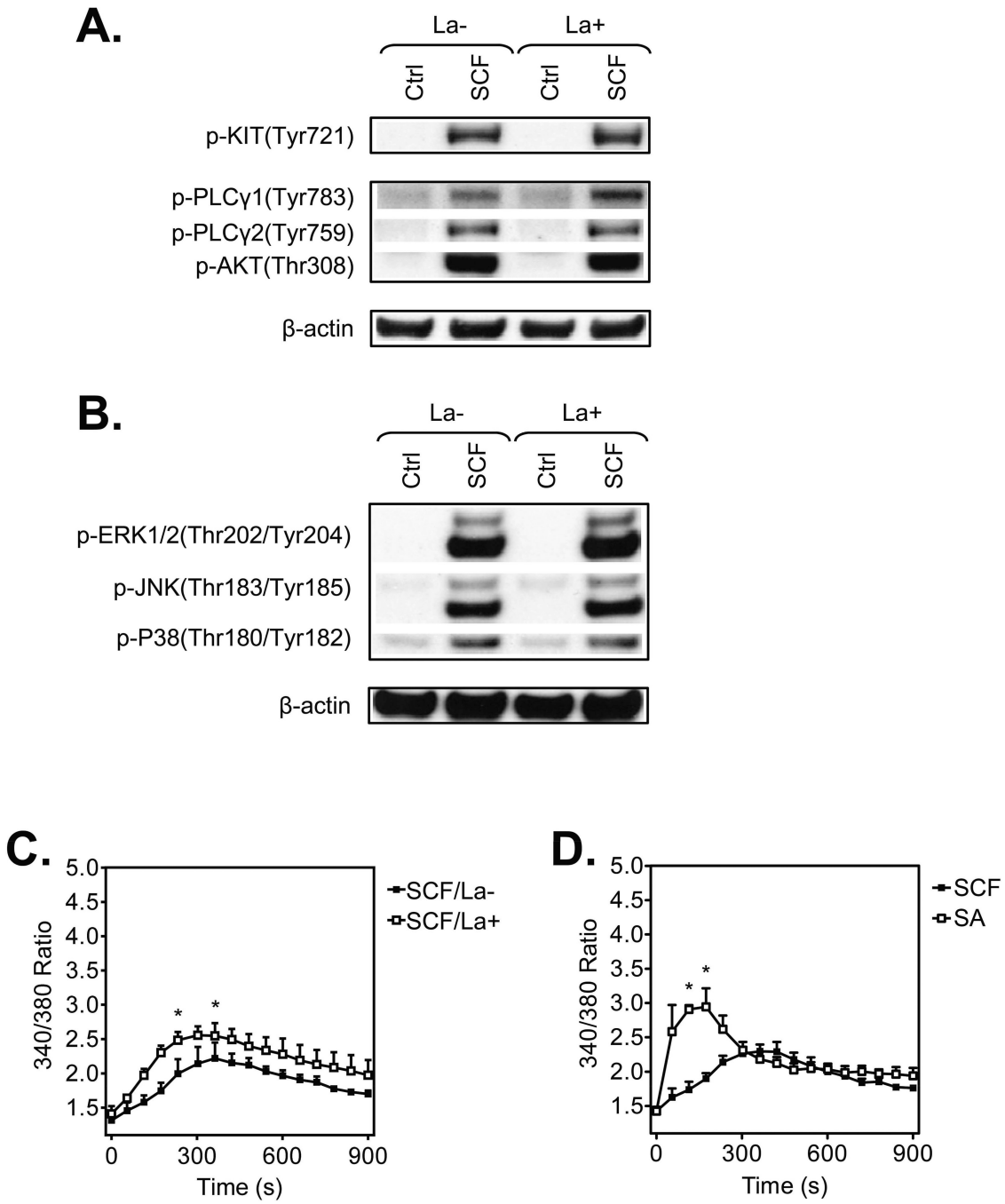

Figure 5.

Impact of inhibition of actin polymerization by latrunculin B in huMCs on early SCF-induced signaling events. (**A–B**) Non-sensitized and cytokine-starved huMCs were pre-treated (La+), or not (La−), with latrunculin B (1 μM) for 20 min, then activated, or not (Ctrl), with SCF (100 ng/ml) for 2 min. The cells were lysed and analyzed by immunoblotting. β-actin was used as a loading control and data shown are from one donor but are representative of immunoblots performed for 3 donors. Quantitative data for all 3 donors are shown in Supporting Information Fig. 1. (**C**) Non-sensitized and starved huMCs were loaded with Fura-2, pre-treated (La+), or not (La−), with latrunculin B (1 μM) for 20

min and then activated with SCF (100 ng/ml) and calcium response was analyzed. (**D**) Sensitized and starved huMCs were loaded with Fura-2, then activated with SCF (100 ng/ml) or SA (100 ng/ml) and calcium response was analyzed. (**C–D**) Data are shown as mean + SEM of n=3 individual donors. *P<0.05, Student's t-test, between latrunculin B-treated and non-treated (**C**) or differentially activated (**D**) cells.

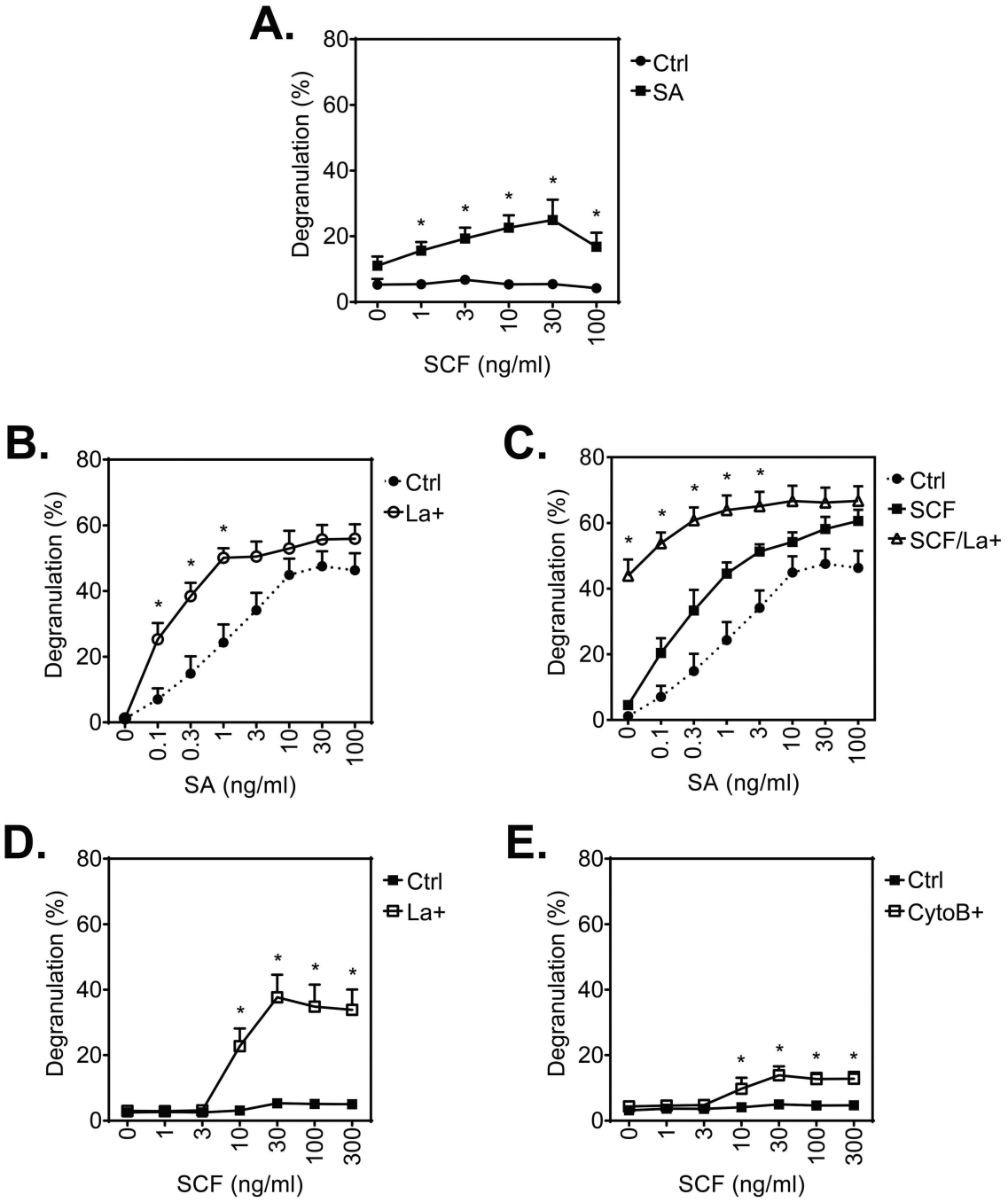

Figure 6.

Effect of inhibition of actin polymerization on huMC degranulation after stimulation with SA and/or SCF. (**A**) Sensitized (bio-huIgE; 100 ng/ml) and starved huMCs were activated with SCF (0–100 ng/ml) in the presence or absence of SA (1 ng/ml) for 30 min and degranulation was determined. (**B**) Sensitized (bio-huIgE) and cytokine-starved huMCs were pre-treated (La+), or not (Ctrl), with latrunculin B (1 μM) for 20 min and then activated with SA (0–100 ng/ml) for 30 min and degranulation was determined. (**C**) Sensitized and cytokine-starved huMCs were pre-treated (La+), or not, with latrunculin B (1 μM) for 20 min and then activated with SA (0–100 ng/ml) in the presence of SCF (100 ng/

ml). Degranulation of the latrunculin B-untreated and SA-stimulated cells from (**A**). (Ctrl) is shown for a comparison. (**D**) Non-sensitized and starved huMCs were pre-treated (La+), or not (Ctrl), with latrunculin B (1 μM) for 20 min and then activated with SCF (0–300 ng/ml) for 30 min and degranulation was determined. (**E**) Non-sensitized and SCF-starved huMCs were pre-treated (CytoB), or not (Ctrl), with cytochalasin B (20 μM) for 20 min and then activated with SCF (0–300 ng/ml) for 30 min and degranulation was determined. Data are shown as mean + SEM of n=4 donors (**A, E**) and n=3 individual donors (**B–D**). *P<0.05, Student's t-test, between differentially stimulated (**A**) or treated (**B–E**) cells.

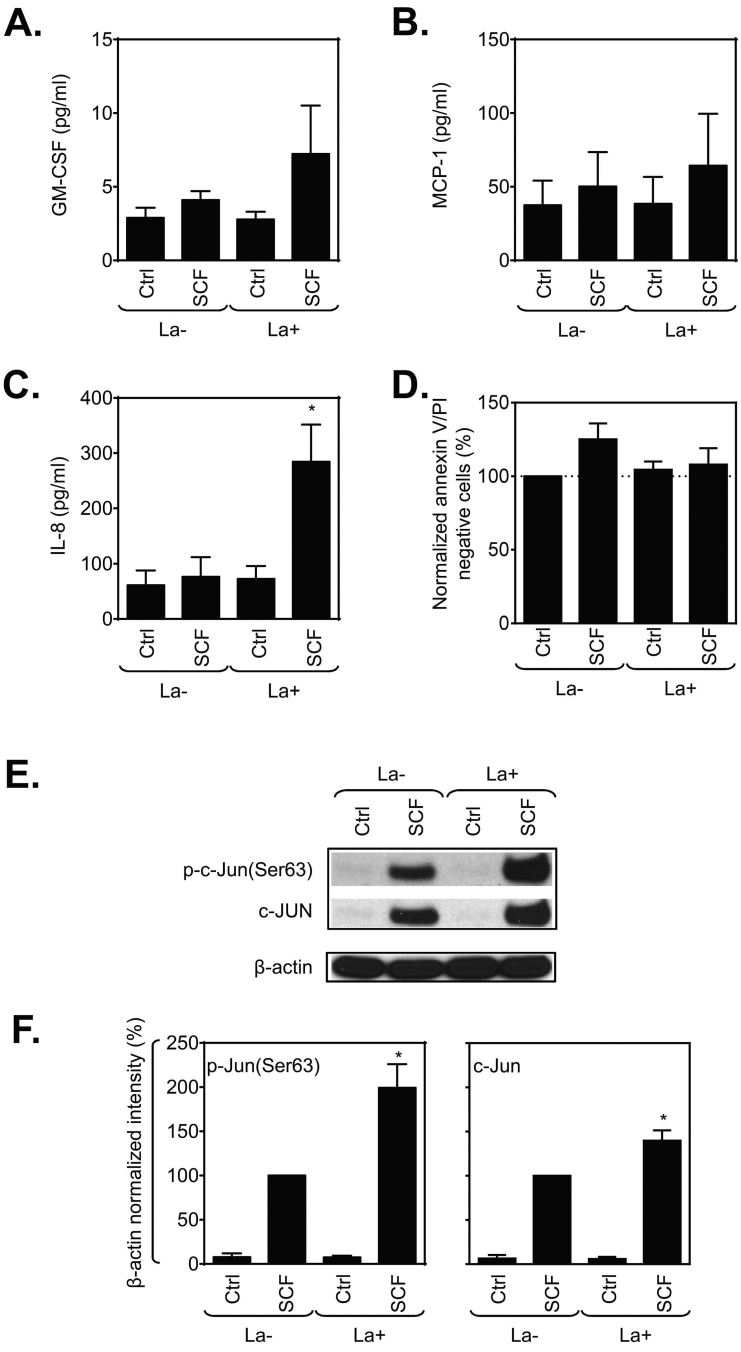

Figure 7.

Inhibition of actin polymerization selectively impacts huMC cytokine production after stimulation with SCF. (**A–C**) Non-sensitized and SCF-starved huMCs were, or not (Ctrl), challenged with SCF (100 ng/ml) for 6 h in cytokine-free media and released cytokines were determined. (**D**) Post-assay viability of cells in (**A–C**) was determined by annexin V/PI staining and flow cytometry, and normalized data were evaluated. (**E**) Typical immunoblots for experiments performed as in (**A–C**) except that cells were sensitized and lysed 30 min after addition of SCF. Quantitative data are shown in (**F**). Data are shown as mean + SEM of

n=3 individual donors. *P<0.05, Student's t-test, between latrunculin B-treated and non-treated, or unstimulated and stimulated cells.